Morphine Regulated Synaptic Networks Revealed by Integrated Proteomics and Network Analysis

Steven D. Stockton Jr. [1, 2], Ivone Gomes[1], Tong Liu[3], Chandrakala Moraje[1], Lucia Hipólito[4], Matthew R. Jones[1], Avi Ma'ayan[1], Jose A. Morón[4], Hong Li[3] and Lakshmi A. Devi[1,2*.]

[1]Department of Pharmacology and Systems Therapeutics, [2]Department of Neuroscience and Friedman Brain Institute, Icahn School of Medicine at Mount Sinai, New York, New York, [3]Center for Advanced Proteomic Research and Department of Biochemistry and Molecular Biology, New Jersey Medical School Cancer Center, Rutgers University, Newark, NJ, [4] Department of Anesthesiology, Columbia University Medical Center, New York, NY.

*Corresponding Author: Lakshmi A. Devi, Ph.D.

Department of Pharmacology and Systems Therapeutics

Icahn School of Medicine at Mount Sinai,

19-84 Annenberg Building

One Gustave L. Levy Place, New York, NY 10029

Phone: (212) 241-8345

Fax: (212) 996-7214

e-mail: lakshmi.devi@mssm.edu

Running Title: Morphine Tolerant Synapse

Abbreviations: ACN, acetonitrile; AMPA, α-amino-3-hydroxy-5-methyl-4-isoxazolepropionic acid; BCA, bicinchoninic acid; CASP3, caspase-3; CREB, cAMP response element-binding protein; CTCF, CCCTC-binding factor; i.p., intraperitoneal; FDR, false discovery rate; FWHM, full-width at half maximum; HCD, higher energy collision dissociation; HSP-70, heat shock protein-70; iTRAQ, isobaric tag for relative and absolute quantitation; LRRK2, leucine-rich repeat kinase2; MALDI, matrix-assisted laser desorption/ionization; MMTS, methyl-methanethiosulfate; MS, mass spectrometry; MSN, medium spiny neuron; NEDD4, neural precursor cell expressed developmentally downregulated protein 4; PAGE, polyacrylamide gel electrophoresis; PPI, protein-protein interaction; PRE, presynaptic density; PSD, postsynaptic density; RIPK, receptor interacting serine/threonine protein kinase; RPLC, reverse phase liquid chromatography; SCXLC, strong cation exchange liquid chromatography; SDS, sodium dodecyl sulfate; TCEP, Tris-(2-carboxyethyl)phosphine; TEAB, triethylammonium bicarbonate; TFA, trifluoroacetic acid; TX-100, Triton X-100; UPS, ubiquitin-proteasomal system; USP8, ubiquitin carboxyl terminal hydrolase 8.

Summary

Despite its efficacy, the use of morphine for the treatment of chronic pain remains limited because of the rapid development of tolerance, dependence and ultimately addiction. These undesired effects are thought to be due to alterations in synaptic transmission and neuroplasticity within the reward circuitry including the striatum. In this study we used subcellular fractionation and quantitative proteomics combined with computational approaches to investigate the morphine-induced protein profile changes at the striatal postsynaptic density. Over 2,600 proteins were identified by mass spectrometry analysis of subcellular fractions enriched in postsynaptic density associated proteins from saline or morphine-treated striata. Among these, the levels of 34 proteins were differentially altered in response to morphine. These include proteins involved in G-protein coupled receptor signaling, regulation of transcription and translation, chaperones, and protein degradation pathways. The altered expression levels of several of these proteins was validated by Western blotting analysis. Using Genes2Fans software suite we connected the differentially expressed proteins with proteins identified within the known background protein-protein interaction network. This led to the generation of a network consisiting of 116 proteins with 40 significant intermediates. To validate this, we confirmed the presence of three proteins predicted to be significant intermediates: caspase-3, receptor-interacting serine/threonine protein kinase 3 and NEDD4 (a E3-ubiquitin ligase identified as a neural precursor cell expressed developmentally downregulated protein 4). Since this morphine-regulated network predicted alterations in proteasomal degradation, we examined the global ubiquitination state of postsynaptic density proteins and found it to be substantially altered. Together, these findings suggest a role for protein degradation and for the ubiquitin/proteasomal system in the etiology of opiate dependence and addiction.

Introduction

Morphine and other opiates are the drugs of choice for the treatment of both severe and chronic pain. However, the utility of these compounds in the clinical setting is limited due to the rapid development of tolerance, physical dependence and addiction. The underlying cellular and molecular alterations through which chronic opiate exposure results in the persistent behavioral phenomenon of addiction remain poorly understood. However, there is evidence suggesting that the molecular composition of synapses within the reward circuitry of the central nervous system, particularly in the striatum, may be significantly altered (1). Moreover, given the critical involvement of the striatum in translating emotional or rewarding stimuli into motivated behaviors, alterations in this region induced by morphine and other abused drugs could contribute significantly to the pathophysiological responses at the heart of addiction (2). Although the debate surrounding the molecular and cellular mechanisms by which repeated drug administration leads to addiction is still continuing, there is substantial evidence for the involvement of synaptic plasticity within the striatum in this process.

Studies show that morphine administration both reduces the complexity of dendritic branching and spine density of striatal medium spiny neurons (MSNs) (3, 4), and causes structural modifications that are known to lead to alterations in synaptic efficacy (1, 4, 5). In addition to these morphological alterations, morphine also regulates the expression of transcription factors that are involved in mechanisms of learning and synaptic plasticity such as CREB (6), ΔFosB (6, 7), and NF-κ-B (8). Prolonged exposure to morphine and other opiates also results in a number of important molecular and electrophysiological changes at synaptic terminals. Thus morphine exposure reduces transmembrane Ca^{2+} conductance and neurotransmitter release (9, 10), causes alterations in glutamatergic transmission (11-13), enhances postsynaptic K^+ conductance and membrane hyperpolarization (14), and leads to significant upregulation of μ-δ opiate receptor heteromers in the striatum and other brain regions (15-17). Given the wide-reaching changes induced by chronic morphine administration it is

important to develop an understanding of how morphine and other abused drugs generate these neuroplastic changes particularly at the synapse.

Proteomic analysis has been used to elucidate both the *in vitro* (18, 19) and *in vivo* (20-26) changes in the protein profiles of synapses that exhibit drug-induced alterations in response to opiate exposure. For example, the use of subcellular fractionation, which allows for the separation and generation of protein fractions selectively enriched in either pre- or postsynaptic proteins (25, 27), in combination with proteomic analysis has revealed that an acute escalating dose of morphine administration produces significant alterations in the postsynaptic density (PSD) associated protein network in the hippocampus. This includes significant redistribution of endocytic proteins such as clathrin (20, 22) and glutamatergic α-amino-3-hydroxy-5-methyl-4-isoxazolepropionic acid (AMPA) receptors (12, 13). Proteomic analysis coupled with tandem mass spectrometry (MS/MS) followed by the computational analysis that placed the proteomics results within known protein-protein interaction (PPI) networks also revealed a novel function for heat shock proteins and their co-chaperones in the presynaptic active zone of the morphine tolerant striatum. This, in turn, led to the identification of a therapeutic target that, when inhibited, prevented the development of tolerance and dependence while preserving the analgesic properties of morphine (24). This illustrates the power of proteomic analysis in combination with tandem mass spectrometry and data analysis that integrates known PPI networks in detecting and predicting protein changes in a specific subcellular fraction.

In this study we used a quantitative subcellular proteomic approach in order to explore morphine-regulated changes in the PSD fraction of the morphine dependent striatum. For this the striata of animals subjected to chronic escalating doses of morphine (28), were subjected to subcellular fractionation (27) so as to obtain fractions enriched in PSD proteins. In order to reveal relative changes in the abundance of PSD-related proteins, PSD fractions from individual morphine and saline treated animals were labeled with the 8-plex isobaric tags for relative and absolute quantitation (iTRAQ), and then subjected to MS/MS analysis. These experiments

5

identified a total of 2,648 proteins, of which 2,643 were quantified. Among these proteins, 34 proteins (~1.4 %) exhibited statistically significant regulation in response to chronic morphine treatment and were named the "High Confidence Morphine Regulated Proteins"; 10 of these proteins were significantly downregulated, while the other 24 proteins were significantly upregulated relative to saline controls. In order to place these differentially expressed proteins within the known biology of the synapse, we used the web-based tool Enrichr (29) for performing protein set enrichment analysis, and Genes2FANs (30) to construct a morphine-regulated subnetwork. Among the proteins identified to be enriched for interactions with the 34 proteins we identified as differentially expressed   at the synpase, we selected caspase-3, receptor-interacting serine/threonine protein kinase 3, and NEDD4 for experimental validation by Western Blotting.   We also found that the global ubiquitination state of the striatal PSD proteins is altered by chronic morphine administration suggesting a broad role for ubiquitination and protein degradation in the development of tolerance to morphine.

Experimental Procedures:

Materials

Rabbit-anti-PSD-95 (Catalog# 2507), rabbit-anti-synaptophysin (Catalog# 5467S), rabbit-anti-Gαo (Catalog# 3975S), rabbit-anti-HSP70 (Catalog# 4872), rabbit-anti-GAP43 (D9C8) (Catalog# 8945), rabbit-anti-USP8 (Catalog# 8728), mouse-anti-Ubiquitin (P4D1) (Catalog# 3936), mouse-anti-Caspase-3 (3G2) (Catalog# 9668), rabbit-anti-NEDD4 (C5F5) (Catalog# 3607) were from Cell Signaling Technology, Danvers, MA, USA. Rabbit-anti-Gβ1 (Catalog# NBP1-55307), and rabbit-anti-Annexin 6 (Catalog# NBP1-80514) were from Novus Biologicals, Littleton, Colorado, USA. Rabbit-anti-PPP3R1/Calcineurin B (Catalog# AP09004PU-N) was from Acris Antibodies GmbH, San Diego, CA, USA. Rabbit-anti-RIPK3 (Catalog# 20R-1514) was from Fitzgerald Industries International, Acton, MA, USA.

For extraction of proteins and iTRAQ labeling the following materials and reagents were used: Tris-(2-carboxyethyl) phosphine (TCEP), methyl-methanethiosulfate (MMTS), mobile Phase A (10 mM KH_2PO_4 with 25% acetonitrile (ACN), pH 3.0), mobile Phase B (500 mM KCl, 10 mM KH_2PO_4 and 25% ACN, pH 3.0), solvent A (5% ACN with 0.1% trifluoroacetic acid (TFA)), solvent B (95% ACN with 0.1% TFA), MALDI matrix solution (7 mg/mK alpha-cyano-4-hydroxycinnamic acid (Sigma-Aldrich, St. Louis, MO, USA) in 60% ACN, 5 mM ammonium monobasic phosphate and 50 fmol/µL of each of the following internal peptidergic calibrants [Glu-1]-Fibrinopeptide B (Glu-Fib, Sigma-Aldrich) and adrenocorticotropic hormone, fragment 18-39 (ACTH (18-39), Sigma-Aldrich).

Research Animals

Adult morphine-naïve male Sprague-Dawley rats (N=4 for control and experimental groups respectively) were maintained on a 12-h light/dark cycle with access to food and water *ad libitum*. All animals were permitted to acclimatize to their environment for approximately one week prior to treatment. All experiments were designed and performed in accordance with the recommendations set forth in the *Guide for the Care and Use of Laboratory Animals: Eighth*

Edition (31), and were approved and monitored by the Institutional Animal Care and Use Committee (IACUC) at the Icahn School of Medicine at Mount Sinai (Protocol #LA11-00322).

Morphine Treatment

Morphine and saline control injections were administered essentially as described previously (2, 24, 28, 32). Morphine sulfate (Sigma-Aldrich, St. Louis, MO, USA) was prepared in 0.9% sterile isotonic solution of saline. All injections were administered intraperitoneally (i.p.), and consisted of 0.9% saline (control group) or escalating doses of morphine (experimental group). For morphine treatment, a chronic escalating morphine administration paradigm (2, 24, 28, 32) was used. Briefly, animals received every 12 h escalating doses of morphine ranging from 5 mg/kg on day 1 to 50 mg/kg on the final day (2, 24, 28, 32). All animals were sacrificed 2 h after the final injection, the striata were rapidly dissected on ice and stored at -80º C until used for subcellular fractionation as described below.

Subcellular Fractionation and Isolation of Postsynaptic Proteins

The striatum from each control and experimental animal was hemisected, and each half used to generate two fractions: a primary sample for use in experiments, and a backup sample to be used in the event of contamination or loss of the primary sample. Each striatal half was subjected to cell fractionation to obtain PSD fractions as described previously (22, 27, 33) (Fig.1A). The pellet containing the PSD fraction was re-suspended in 200-250 µL of 1% SDS, the amount of protein determined using the BCA protein estimation kit (Thermo Scientific Pierce, Rockford, IL, USA), and stored at -80º C until use.

Immunoblotting

Homogenate or PSD fractions (15 µg protein) from morphine or saline treated animals were resolved by 7.5% SDS-PAGE, and transferred to nitrocellulose membranes (Schleicher & Schuell Bioscience, Keene, NH, USA). Membranes were incubated with primary antibodies for 24 h on an orbital shaker at 4º C at dilutions recommended by the manufacturer. Following four washes (15 min each) at room temperature with 50 mM Tris-Cl pH 7.4 containing 150 mM NaCl,

1 mM CaCl$_2$ and 0.1% Tween 20 (TBS-T) membranes were incubated in 1:10,000 dilution of either IR800CW- or IR680-labeled goat anti-mouse or anti-rabbit secondary antibodies (LI-COR Biosciences, Lincoln, NE, USA). Membranes were washed 4 times (15 min each) at room temperature with TBS-T and protein bands were visualized and densitized using the Odyssey infrared imaging system (LI-COR Biosciences).

Protein Extraction and iTRAQ Labeling

PSD fractions were subjected to iTRAQ as described previously (20, 34, 35). Briefly, 100 µg of protein from each saline and morphine treated sample was subjected to SDS-PAGE. The gel was then fixed, stained and rinsed with 25 mM triethylammonium bicarbonate buffer (TEAB) to remove SDS and Tris. The proteins were reduced in the presence of Tris(2-carboxyethyl)phosphine hydrochloride (TCEP), followed by alkylation with methylmethanethiosulfonate (MMTS) (ABSciex, Foster City, CA, USA), and in-gel trypsin digestion (Promega, Madison, WI, USA) overnight at 37º C. The peptides were extracted with 25 mM TEAB followed by 80% acetonitrile. The peptides were concentrated using a speed-vac and their pH adjusted to 8.5 with 500 mM TEAB. The iTRAQ labeling was performed according to the manufacturer's protocol using the following isobaric iTRAQ tags: 113, 114, 115 and 116 tags for saline control samples, and 117, 118, 119 and 121 tags for morphine treated samples (ABSciex). After incubation with the iTRAQ tags at room temperature for 2 h, the iTRAQ labeled peptides from saline and morphine treated samples were combined and subjected to strong cation exchange liquid chromatography (SCXLC): a polysulfoethyl A strong cation exchange column (4.6mm x 200mm, 5µm, 300Å, Poly LC Inc., Columbia, MD, USA) on a BioCAD SPRINT Perfusion chromatography system (PerSeptive Biosystems Inc., Framingham, MA, USA) that was coupled to an upstream guard column (4.0mm x 10mm, Poly LC Inc.) was used. Separation of the different iTRAQ labeled striatal PSD peptides was achieved across a gradient of mobile Phase A (10 mM KH2PO4 in 25% acetonitrile, pH 3) and mobile Phase B (0.6 M KCl and 10 mM KH2PO4 in 25% acetonitrile, pH 3) containing two linear segments: 40

min from 0-50% B, followed by 10 min from 50-100% B at a flow rate of 1 ml/min. Twenty eluted fractions were collected, dried completely with a speed-vac, and desalted using PepClean™ C_{18} spin columns (Pierce, Rockford, IL, USA).

Tandem Mass Spectrometric (MS/MS) Analysis

Peptides from SCXLC fractions were further analyzed by RPLC-MS/MS on Obitrap Velos mass spectrometer. Briefly, peptides were loaded onto a reversed phase trapping column (0.3 mm x 5.0 mm), and subsequently resolved on a capillary C_{18} PepMap column (0.1mm x 150 mm, 3 µm, 100 Å, Dionex). Peptides were eluted using a 70 min gradient of solvent A and solvent B as follows: 5% to 8% B from 0-4 min, 18% B at 34 minutes, 35% B at 57 minutes, and 95% B at 64 minutes. The eluted peptides were introduced into a nano electrospray source on Obitrap Velos MS system with a spray voltage of 2 kV, a capillary temperature of 275 ^{0}C and a S-lens voltage of 60%. MS spectra were acquired in a positive ion mode with a resolution of 60,000 full-width at half maximum (FWHM). The Higher Energy Collision Dissociation (HCD) MS/MS spectra were acquired in a data-dependent manner. The 10 most abundant ions were selected for HDC fragmentation per MS scan in the Orbitrap at a resolution of 7500 FWHM. The normalized collision energy was set to 40. The lock mass feature was engaged for accurate mass measurements.

Identification and Quantification of Proteins

The MS/MS spectra were searched against UniRef 100 rat database (51,862 entries) using both Mascot (v.2.3) and Sequest search engines via the Proteome Discoverer platform (v 1.3; Thermo Scientific). In conducting this search, the following search parameters were used: (i) fixed modifications included iTRAQ 8plex (K), iTRAQ 8plex (N-terminal), and methylthio (C); (ii) variable modifications included iTRAQ 8plex (Y) and oxidation (M); (iii) trypsin was selected as the digestive enzyme; (iv) a maximum of one missed cleavage site was allowed; (v) the peptide precursor mass tolerance was 10 ppm; and (vi) MS/MS mass tolerance was 0.1 Da. Scaffold (v.3.6.3, Proteome Software Inc., Portland, OR) was used to validate MS/MS based

peptide and protein identification. Peptide identifications were accepted if they could be established at ≥ 90% probability by Peptide Prophet (36). A false discovery rate (FDR) was maintained at < 1%. Similarly, protein identifications were accepted if they could be established at ≥ 95% probability and contained at least 1 uniquely identified peptide. Protein probabilities were assigned by the Protein Prophet Algorithm (37). Protein FDR was maintained at < 1%. Homologous protein redundancy was reduced by Scaffold software (V. 3.0) in a minimum. Proteins that contained similar peptides and could not be differentiated based on MS/MS analysis alone were grouped to satisfy the principles of parsimony.

Quantitative values obtained for each identified protein were determined based only on unique peptides that were detected and assigned to each respective protein. Quantitative ratios for a given protein from each of the saline or morphine treated samples (Table S1) were calculated as the average of all unique peptide ratios that were associated with a given protein. All quantitative ratios were Log_2 normalized for the final quantitative analysis. Proteins with a t-test value of $p<0.05$ and with a morphine to saline ratio greater than 1.2 fold or less than 0.8 fold were considered as significantly changed.

Enrichment Analysis of Proteomic Data and Generation of Protein-Protein Interaction Networks

The lists of significantly altered proteins were first subjected to gene set enrichment analysis using the tool Enrichr (29). Enrichr uses the Fisher exact test to compute enrichment. In order to generate a PPI network based on proteins identified by proteomics as being modified by morphine treatment we generated a "*Morphine Seed List*" (53 morphine regulated and altered proteins; 38 upregulated and 15 downregulated proteins). This list was created by combining a "*High Confidence Morphine Regulated Proteins*" dataset (38 significantly altered proteins (p < 0.05); 24 upregulated and 10 downregulated proteins) (Table 1 & 2) with a "*Low Confidence Morphine Regulated Proteins*" dataset (19 morphine altered proteins (p <0.1); 14 upregulated and 5 downregulated proteins) (Table S2). The proteins in the "*Morphine Seed List*" were connected using the PPI module of Genes2FANs, a web-based software tool (30, 38), that

11

integrates 13 mammalian binary interaction network datasets including HPRD, IntAct, KEGG, MINT, and BioGrid (38). The integration of these datasets results in a background PPI network that contains 11,053 proteins connected through 44,985 direct PPIs. To increase the reliability of the interactions, we only retained interactions arising from sources that contributed five or more PPIs. The proteins from the "*Morphine Seed List*" were then connected to each other using the shortest path algorithm with a maximum path length of three. Once the construction of the PPI subnetwork using Genes2 FANs (30) was complete the finalized network was then visualized using Cytoscape v2.8.3 (39).

The Genes2FANs software prioritizes intermediate proteins that connect the seed list of input proteins using the Binomial proportion test. Predicted intermediates with a Z-score > 3 were deemed "highly significant intermediates", between 2 and 3 "significant intermediates", and < 2 "intermediates". The presence of potential clusters within the generated PPI network was assessed with Cfinder (40). Cfinder utilizes the clique percolation method to localize k-clique percolation clusters within the network.

Results

The present study seeks to elucidate alterations in striatal PSD protein expression in response to prolonged exposure to morphine using a combination of proteomics and network biology. For this animals were treated with either saline or escalating doses of morphine for 5 days (2, 24, 28, 32). The striatum of individual animals was rapidly dissected out and subjected to subcellular fractionation (Fig. 1A) in order to isolate the selectively enriched PSD associated protein fraction (22, 25, 27, 33). The enrichment of PSD associated proteins in this fraction was verified by Western blot analysis using antibodies directed against well-characterized presynaptic (synaptophysin) and postsynaptic (PSD-95) markers. In the case of synaptophysin we detect a strong signal in homogenate fractions from both saline and morphine treated animals but no detectable signal was observed in the PSD fractions of these animals (Fig. 1B). In the case of PSD-95, the intensity of the signal was much stronger in the PSD fractions compared to the homogenate in both saline and morphine treated animals (Fig. 1B). These results indicate that our striatal PSD preparations are enriched in PSD-associated proteins.

Next, we identified changes in the protein profile of the striatal PSD fractions following morphine treatment. This was achieved by labeling peptide fragments from four saline and four morphine treated animals with 8-plex iTRAQ reagents, mixing the labeled peptides and subjecting the peptide mixture to LC-MS/MS analysis. This led to the identification of 2,648 unique proteins in the striatal PSD fractions (Table S1), of which 2,643 were reliably quantified (see "*Experimental Procedures*"). Representative spectra illustrating the identification and quantification of two distinct proteins detected in this study (synaptopodin which was decreased by morphine treatment and Gαo which was increased) are shown in Fig. 2.

Among the proteins identified by LC-MS/MS analysis, a total of 34 (~1.4%) exhibited greater than a 20% change ($p < 0.05$; t-test) in the samples from morphine treated animals relative to the saline controls. These proteins, of which 24 were significantly upregulated and 10 were significantly downregulated in response to morphine treatment, were labeled as "*High*

13

Probability Morphine Regulated Proteins" (Table 1 & 2). Interestingly, among the identified "*High Probability Morphine Regulated Proteins*" were a number of signaling molecules, calcium-binding proteins, as well as proteins from the ubiquitin-proteosomal system (UPS). Next, we confirmed by Western blot analysis the changes in the expression levels of several proteins suggested by MS/MS analysis to be significantly altered following morphine treatment. These included up-regulated proteins such as guanine-nucleotide binding protein Gαo, guanine-nucleotide binding protein Gβ1, calcineurin subunit B Type 1, neuromodulin, annexin-VI, and heat shock protein-70 (HSP-70) (Fig. 3) as well as down-regulated proteins such as ubiquitin carboxyl terminal hydrolase 8 (USP8) (Fig.4A). We found that the decreased abundance of USP8 in the striatial PSD fractions of morphine treated animals was accompanied by a significant increase in total levels of ubiquitinated proteins (Fig. 4B).

Next we performed a protein set enrichment analysis using the tool Enrichr (29), and relevant gene set libraries such as mammalian phenotypes for knockout mice, Reactome pathways, Human Gene Atlas, ENCODE and TargetScan. The results show that both the upregulated and downregulated proteins are enriched for neuronal defect phenotypes (Fig. 5). Reactome enrichment analysis suggest an increase in opioid signaling components which are likely to be an adaptive mechanism (Fig. 5). Interestingly, many of the upregulated proteins are targets of two microRNA family members, whereas the downregulated proteins are enriched in genes highly expressed in the pineal gland and regulated by the transcription factor CTCF (Fig. 5).

Next we generated a PPI network based on proteins modified by morphine treatment using the Genes2Fans software suite (30). For this we generated a *"Morphine Regulated Protein Seed List"* (further referred to simply as the "seed list") by combining the observed "*High Probability Morphine Regulated Proteins*" (Table 1 & 2) with a set of proteins that exhibited lower levels of statistical significance ($0.05 < p < 0.10$), defined as the "*Low Probability Morphine Regulated Proteins*" (Table S2). We used Genes2Fans to connect as many pairs of

seed list proteins as possible using intermediate proteins interactions identified within the known background PPI network. This allowed us to obtain a PPI subnetwork that comprised a total of 116 proteins, 17 from the seed list and 93 from the background PPI network (Table 3 shows the list of Significant intermediates). These proteins were connected via 223 identified interactions (Fig. 6). Genes2Fans applied a binomial proportions test to prioritize the additional proteins that connect our seed list and found 40 significant intermediate proteins (Z-score > 2.0). Among these 40 proteins, 28 were found to be highly significant intermediates (Z-score > 3) while 12 were identified as significant intermediates ($2.0 \leq$ Z-score ≤ 3.0). We also carried out cluster analysis using CFinder (v.2.0.5) (40, 41). Cluster analyses showed that our network exhibited a higher clustering coefficient (0.169, p<0.01) compared to 100 scrambled networks generated from the background dataset that had identical network topology (clustering coefficient of 0.086) which suggests a degree clustering that is distinctly non-random. Interestingly, our network predicts a number of receptors including opioid receptors, signaling molecules involved in calcium signaling as well as molecules whose function at the PSD is not as yet known as significant intermediates. Next, we validated the predicted significant intermediate proteins by Western blot analysis. For this we selected three of the most unique proteins identified by Genes2FANs as none of them were known to localize to, or function at, mature synapses prior to this investigation: caspase-3 (CASP3), receptor interacting serine/threonine protein kinase 3 (RIPK3), and the E3-ubiquitin ligase neural precursor cell expressed developmentally down-regulated protein 4 (or NEDD4). Western blot analysis using synaptosomal fractions showed that the expression levels of RIPK3 and CASP3 tended to decrease in morphine treated animals while levels of NEDD4 were significantly decreased compared to saline treated controls (Fig. 7).

15

Discussion

The present study utilized a combination of subcellular fractionation (22, 25, 27, 33), quantitative proteomic approaches and network analysis in an effort to examine alterations in the postsynaptic protein profile within the striatum as a consequence of prolonged exposure to morphine. Of the 2,648 proteins that were identified in this study, 34 (or ~1.4% of the proteins identified) exhibited significantly altered expression following the morphine treatment paradigm. Among these 34 morphine-regulated proteins, 24 exhibited significant upregulation (Table 1), while the remaining 10 were significantly downregulated (Table 2)*.* Among the proteins upregulated following morphine treatment were proteins involved in G-protein signaling, including $G\alpha_O$, $G\beta1$, and $G\beta2$. These results are in agreement with previous studies that showed increased expression of G-protein subunits particularly $G\alpha_O$ and $G\alpha_i$ during opiate addiction (42, 43) in a number of neuroanatomical regions including the prefrontal corted, locus coeruleus and nucleus accumbens (44). This effect of morphine could extend to the molecular level, since an increased synthesis of $G\alpha_O$ and a decrease in the synthesis of $G\alpha_S$ was observed in the rodent hippocampus subsequent to chronic morphine exposure (45). Interestingly, proteomic studies using hippocampal PSD fractions of mice treated with escalating doses of morphine reported a slight (0.92 fold) decrease in the abundance of a closely related G-protein subunit, $G\alpha_{O2}$, compared to saline treated controls (22).

In this study we find that among the striatal postsynaptic proteins altered by morphine administration are several that are associated with the Ubiquitin-Proteasome System (UPS) such as PRAJA-1, FAM160A2, ubiquitin carboxyl-terminal hydrolase 8 (USP8), and ATG7. Of these Praja-1, FAM160A2, and USP8 were downregulated while ATG7 was upregulated in morphine treated animals. Interestingly a previous proteomics study investigating changes in phosphotyrosinated proteins in the frontal cortex of morphine dependent animals also detected alterations in a number of UPS related proteins (43). To date very little is known about the role of these proteins in the central nervous system. PRAJA-1 is a E2-dependent E3 ubiquitin ligase

16

that is abundantly expressed in the brain (46), and has as its putative substrates the postsynaptic proteins Homer2, CAMK1G, EPHB3 and SEPT1 (47). PRAJA-1 has been implicated in learning and memory associated with fear conditioning (48). FAM160A2 is a FHIP protein that is a component of the FTS and Hook-interacting protein/FHIP (FHF) complex (49). The FTS component of the complex is an E2 ubiquitin-conjugating enzyme (49) and the complex as a whole has been implicated in sorting to early endosomes (50). ATG7 has been shown to be involved in autophagy, a process that can be recruited to clear aggregated ubiquitin-tagged proteins following USP disruption (51). USP8, also known as USPγ or HUMORF8, is a deubiquitinating hydrolase that regulates protein turnover by removing ubiquitin from proteins targeted for degradation (52). USP8 has been shown to regulate the surface expression, endocytosis and degradation of a number of channels and receptors including the delta opioid receptor (53-57). Interestingly, in this study we find that morphine treatment leads to a decrease in the expression of USP8 in striatal PSD fractions and this is accompanied by a significant increase in the total levels of ubiquitinated proteins. This would suggest an UPS involvement in the development of tolerance and dependence to morphine. Thus, further studies are needed to evaluate the role of ubiquitinating and deubiquitinating enzymes in drug addiction.

The PPI network generated by Genes2FANs predicts caspase-3, RIPK3 and NEDD4 as significant intermediates in morphine induced changes at striatal PSDs; however, very little is known about the role of these proteins at the synapse during addiction to morphine. Caspase-3 (CASP3), which we find in this study to be decreased in synaptosomal fractions of morphine treated animals, is best known for its role during apoptosis as an executioner caspase that leads to neuronal cell death (58, 59). However, recent studies have revealed not only developmental functions but also a functional role for this enzyme in the regulation of synaptic plasticity, learning, and memory (60). Studies have demonstrated the presence of caspase-3 in both dendrites and PSD fractions (61), and have shown that it can modulate synaptic transmission by interacting with and cleaving specific AMPA subunits at the PSD (62), and by regulating the

17

internalization of synaptic AMPA receptors (63). In this context, it is interesting to note that both caspase-3 and NEDD4 (another significant intermediate protein predicted by Genes2FANs) have been shown to modulate AMPA receptor surface expression through their interactions with the GluR1 subunit (63). In addition, caspase-3 and NEDD4 have been shown to modulate the activity of E2- and E3-ubiquitin ligases of the ubiquitin-proteasome system (61, 64), some of which were found to be altered in this study following morphine administration. Therefore caspase-3 may play an inportant role in neurological disorders. This is supported by studies that implicate interactions between caspase-3 and glutamate receptors in Alzheimer's disease (65), as well as studies showing that mutations in leucine-rich repeat kinase2 (LRRK2) render dopaminergic neurons more sensitive to caspase-3 activation in Parkinson's disease (66). Although the current study indicates that chronic morphine treatment causes a decrease in the levels of caspase-3, further studies are needed to elucidate the role on this enzyme both at the protein level as well as with regards to its enzymatic activity in the development of tolerance and addiction to drugs of abuse.

Another protein predicted to have a significant involvement in morphine-mediated changes at the striatal PSD is the receptor interacting protein kinase 3 (RIPK3) (Fig. 6 & 7). RIPK3 and the closely related protein RIPK1, are important regulatory proteins involved in the process of necroptosis, a process associated with programmed necrotic cell death (67). Necroptosis is negatively regulated by caspase-8 (67); thus decreased levels of caspase-8 can lead to either RIPK1-dependent or independent mechanisms of recruitment of RIPK3 (67, 68). To date very little information is available about the the role of necroptosis in the central nervous system with one study reporting that 5-aminolevulinic acid-based photodynamic therapy stimulates necroptosis in glioblastomas by increasing the formation of necrosomes enriched in RIPK3 and RIPK1, but lacking other common proteinacious components such as FADD and caspase-8 (69). Thus further studies are needed to elucidate the role of RIPK3 in the brain particularly during the development of tolerance to drugs of abuse.

18

Another interesting protein predicted to be a significant intermediate in this study is neural precursor cell expressed, developmentally downregulated 4 (NEDD4). NEDD4 was first characterized as a developmentally regulated protein with peak expression during early neurogenesis, followed by substantially decreased expression throughout postnatal development (70). NEDD4 is also known to function as an E3 ubiquitin ligase (71) and has recently been reported to contribute to several mechanisms associated with synaptic plasticity in the nervous system. For example, NEDD4-dependent ubiquitination of AMPA receptors bearing GluR1 subunits has been shown to regulate receptor localization, stability, endocytosis and trafficking to lysosomes (72, 73). Interestingly, studies have demonstrated the involvement of AMPA receptors in the persistent synaptic changes following repeated morphine administration (13) as well as increased internalization of AMPA receptors in a clathrin-dependent manner following morphine administration (22). Thus further studies are needed to evaluate the role of NEDD4 in the development of tolerance and dependence to drugs of abuse.

Taken together, this study demonstrates how a combination of proteomics in combination with network analysis can be a powerful tool to detect changes at the striatal synapse following chronic morphine administration and help predict novel proteins that could be potential therapeutic targets to diminish the side-effects associated with chronic morphine use such as the development of tolerance, dependence and addiction.

References:

1.   Russo, S. J., Dietz, D. M., Dumitriu, D., Morrison, J. H., Malenka, R. C., and Nestler, E. J. (2010) The addicted synapse: mechanisms of synaptic and structural plasticity in nucleus accumbens. *Trends Neurosci* 33, 267-276.

2.   Huang, N. K., Tseng, C. J., Wong, C. S., and Tung, C. S. (1997) Effects of acute and chronic morphine on DOPAC and glutamate at subcortical DA terminals in awake rats. *Pharmacol Biochem Behav* 56, 363-371.

3.   Robinson, T. E., and Kolb, B. (1999) Morphine alters the structure of neurons in the nucleus accumbens and neocortex of rats. *Synapse* 33, 160-162.

4.   Grueter, B. A., Rothwell, P. E., and Malenka, R. C. (2012) Integrating synaptic plasticity and striatal circuit function in addiction. *Curr Opin Neurobiol* 22, 545-551.

5.   Luscher, C., and Malenka, R. C. (2011) Drug-evoked synaptic plasticity in addiction: from molecular changes to circuit remodeling. *Neuron* 69, 650-663.

6.   Chao, J., and Nestler, E. J. (2004) Molecular neurobiology of drug addiction. *Annu Rev Med* 55, 113-132.

7.   Perrotti, L. I., Weaver, R. R., Robison, B., Renthal, W., Maze, I., Yazdani, S., Elmore, R. G., Knapp, D. J., Selley, D. E., Martin, B. R., Sim-Selley, L., Bachtell, R. K., Self, D. W., and Nestler, E. J. (2008) Distinct patterns of DeltaFosB induction in brain by drugs of abuse. *Synapse* 62, 358-369.

8.   Nestler, E. J. (2001) Molecular basis of long-term plasticity underlying addiction. *Nat Rev Neurosci* 2, 119-128.

9.   Lovinger, D. M., Partridge, J. G., and Tang, K. C. (2003) Plastic control of striatal glutamatergic transmission by ensemble actions of several neurotransmitters and targets for drugs of abuse. *Ann N Y Acad Sci* 1003, 226-240.

10.   Lovinger, D. M. (2010) Neurotransmitter roles in synaptic modulation, plasticity and learning in the dorsal striatum. *Neuropharmacology* 58, 951-961.

11.   Xu, N. J., Bao, L., Fan, H. P., Bao, G. B., Pu, L., Lu, Y. J., Wu, C. F., Zhang, X., and Pei, G. (2003) Morphine withdrawal increases glutamate uptake and surface expression of glutamate transporter GLT1 at hippocampal synapses. *J Neurosci* 23, 4775-4784.

12.   Billa, S. K., Liu, J., Bjorklund, N. L., Sinha, N., Fu, Y., Shinnick-Gallagher, P., and Moron, J. A. (2010) Increased insertion of glutamate receptor 2-lacking alpha-amino-3-hydroxy-5-methyl-4-isoxazole propionic acid (AMPA) receptors at hippocampal synapses upon repeated morphine administration. *Mol Pharmacol* 77, 874-883.

13.   Xia, Y., Portugal, G. S., Fakira, A. K., Melyan, Z., Neve, R., Lee, H. T., Russo, S. J., Liu, J., and Moron, J. A. (2011) Hippocampal GluA1-containing AMPA receptors mediate context-dependent sensitization to morphine. *J Neurosci* 31, 16279-16291.

14.   Faber, E. S., and Sah, P. (2004) Opioids inhibit lateral amygdala pyramidal neurons by enhancing a dendritic potassium current. *J Neurosci* 24, 3031-3039.

15.   Gupta, A., Mulder, J., Gomes, I., Rozenfeld, R., Bushlin, I., Ong, E., Lim, M., Maillet, E., Junek, M., Cahill, C. M., Harkany, T., and Devi, L. A. (2010) Increased abundance of opioid receptor heteromers after chronic morphine administration. *Sci Signal* 3, ra54.

16.   Stockton, S. D., Jr., and Devi, L. A. (2012) Functional relevance of mu-delta opioid receptor heteromerization: a role in novel signaling and implications for the treatment of addiction disorders: from a symposium on new concepts in mu-opioid pharmacology. *Drug Alcohol Depend* 121, 167-172.

17.   Costantino, C. M., Gomes, I., Stockton, S. D., Lim, M. P., and Devi, L. A. (2012) Opioid receptor heteromers in analgesia. *Expert Rev Mol Med* 14, e9.

18. Bodzon-Kulakowska, A., Suder, P., Mak, P., Bierczynska-Krzysik, A., Lubec, G., Walczak, B., Kotlinska, J., and Silberring, J. (2009) Proteomic analysis of striatal neuronal cell cultures after morphine administration. *J Sep Sci* 32, 1200-1210.

19. Suder, P., Bodzon-Kulakowska, A., Mak, P., Bierczynska-Krzysik, A., Daszykowski, M., Walczak, B., Lubec, G., Kotlinska, J. H., and Silberring, J. (2009) The proteomic analysis of primary cortical astrocyte cell culture after morphine administration. *J Proteome Res* 8, 4633-4640.

20. Prokai, L., Zharikova, A. D., and Stevens, S. M., Jr. (2005) Effect of chronic morphine exposure on the synaptic plasma-membrane subproteome of rats: a quantitative protein profiling study based on isotope-coded affinity tags and liquid chromatography/mass spectrometry. *J Mass Spectrom* 40, 169-175.

21. Abul-Husn, N. S., and Devi, L. A. (2006) Neuroproteomics of the synapse and drug addiction. *J Pharmacol Exp Ther* 318, 461-468.

22. Moron, J. A., Abul-Husn, N. S., Rozenfeld, R., Dolios, G., Wang, R., and Devi, L. A. (2007) Morphine administration alters the profile of hippocampal postsynaptic density-associated proteins: a proteomics study focusing on endocytic proteins. *Mol Cell Proteomics* 6, 29-42.

23. Li, K. W., Jimenez, C. R., van der Schors, R. C., Hornshaw, M. P., Schoffelmeer, A. N., and Smit, A. B. (2006) Intermittent administration of morphine alters protein expression in rat nucleus accumbens. *Proteomics* 6, 2003-2008.

24. Abul-Husn, N. S., Annangudi, S. P., Ma'ayan, A., Ramos-Ortolaza, D. L., Stockton, S. D., Jr., Gomes, I., Sweedler, J. V., and Devi, L. A. (2011) Chronic morphine alters the presynaptic protein profile: identification of novel molecular targets using proteomics and network analysis. *PLoS One* 6, e25535.

25. Bu, Q., Yang, Y., Yan, G., Hu, Z., Hu, C., Duan, J., Lv, L., Zhou, J., Zhao, J., Shao, X., Deng, Y., Li, Y., Li, H., Zhu, R., Zhao, Y., and Cen, X. (2012) Proteomic analysis of the nucleus

accumbens in rhesus monkeys of morphine dependence and withdrawal intervention. *J Proteomics* 75, 1330-1342.

26.	Freeman, W. M., and Hemby, S. E. (2004) Proteomics for protein expression profiling in neuroscience. *Neurochem Res* 29, 1065-1081.

27.	Phillips, G. R., Huang, J. K., Wang, Y., Tanaka, H., Shapiro, L., Zhang, W., Shan, W. S., Arndt, K., Frank, M., Gordon, R. E., Gawinowicz, M. A., Zhao, Y., and Colman, D. R. (2001) The presynaptic particle web: ultrastructure, composition, dissolution, and reconstitution. *Neuron* 32, 63-77.

28.	Trang, T., Sutak, M., Quirion, R., and Jhamandas, K. (2003) Spinal administration of lipoxygenase inhibitors suppresses behavioural and neurochemical manifestations of naloxone-precipitated opioid withdrawal. *Br J Pharmacol* 140, 295-304.

29.	Chen, E. Y., Tan, C. M., Kou, Y., Duan, Q., Wang, Z., Meirelles, G. V., Clark, N. R., and Ma'ayan, A. (2013) Enrichr: interactive and collaborative HTML5 gene list enrichment analysis tool. *BMC bioinformatics* 14, 128.

30.	Dannenfelser, R., Clark, N. R., and Ma'ayan, A. (2012) Genes2FANs: connecting genes through functional association networks. *BMC bioinformatics* 13, 156.

31.	Council, N. R. (2011) *Guide fo the Care and Use of Laboratory Animals: Eight Edition*, Tha National Academies Press, Washington, DC.

32.	Thollander, M., Hellstrom, P. M., and Svensson, T. H. (1989) Suppression of small intestinal motility and morphine withdrawal diarrhoea by clonidine: peripheral site of action. *Acta Physiol Scand* 137, 385-392.

33.	Jordan, B. A., Fernholz, B. D., Boussac, M., Xu, C., Grigorean, G., Ziff, E. B., and Neubert, T. A. (2004) Identification and verification of novel rodent postsynaptic density proteins. *Mol Cell Proteomics* 3, 857-871.

34.   Tyler, W. A., Jain, M. R., Cifelli, S. E., Li, Q., Ku, L., Feng, Y., Li, H., and Wood, T. L. (2011) Proteomic identification of novel targets regulated by the mammalian target of rapamycin pathway during oligodendrocyte differentiation. *Glia* 59, 1754-1769.

35.   Jain, M. R., Li, Q., Liu, T., Rinaggio, J., Ketkar, A., Tournier, V., Madura, K., Elkabes, S., and Li, H. (2012) Proteomic identification of immunoproteasome accumulation in formalin-fixed rodent spinal cords with experimental autoimmune encephalomyelitis. *J Proteome Res* 11, 1791-1803.

36.   Keller, A., Nesvizhskii, A. I., Kolker, E., and Aebersold, R. (2002) Empirical statistical model to estimate the accuracy of peptide identifications made by MS/MS and database search. *Anal Chem* 74, 5383-5392.

37.   Nesvizhskii, A. I., Vitek, O., and Aebersold, R. (2007) Analysis and validation of proteomic data generated by tandem mass spectrometry. *Nat Methods* 4, 787-797.

38.   Berger, S. I., Posner, J. M., and Ma'ayan, A. (2007) Genes2Networks: connecting lists of gene symbols using mammalian protein interactions databases. *BMC bioinformatics* 8, 372.

39.   Smoot, M. E., Ono, K., Ruscheinski, J., Wang, P. L., and Ideker, T. (2011) Cytoscape 2.8: new features for data integration and network visualization. *Bioinformatics* 27, 431-432.

40.   Adamcsek, B., Palla, G., Farkas, I. J., Derenyi, I., and Vicsek, T. (2006) CFinder: locating cliques and overlapping modules in biological networks. *Bioinformatics* 22, 1021-1023.

41.   Derenyi, I., Palla, G., and Vicsek, T. (2005) Clique percolation in random networks. *Phys Rev Lett* 94, 160202.

42.   Terwilliger, R. Z., Beitner-Johnson, D., Sevarino, K. A., Crain, S. M., and Nestler, E. J. (1991) A general role for adaptations in G-proteins and the cyclic AMP system in mediating the chronic actions of morphine and cocaine on neuronal function. *Brain Res* 548, 100-110.

43.   Kim, S. Y., Chudapongse, N., Lee, S. M., Levin, M. C., Oh, J. T., Park, H. J., and Ho, I. K. (2005) Proteomic analysis of phosphotyrosyl proteins in morphine-dependent rat brains. *Brain Res Mol Brain Res* 133, 58-70.

44.   Abul-Husn, N. S., Bushlin, I., Moron, J. A., Jenkins, S. L., Dolios, G., Wang, R., Iyengar, R., Ma'ayan, A., and Devi, L. A. (2009) Systems approach to explore components and interactions in the presynapse. *Proteomics* 9, 3303-3315.

45.   Przewlocka, B., Lason, W., and Przewlocki, R. (1994) The effect of chronic morphine and cocaine administration on the Gs and Go protein messenger RNA levels in the rat hippocampus. *Neuroscience* 63, 1111-1116.

46.   Yu, P., Chen, Y. W., Tagle, D. A., and Cai, T. (2002) PJA1, encoding a RING-H2 finger ubiquitin ligase, is a novel human X chromosome gene abundantly expressed in brain. *Genomics* 79, 869-874.

47.   Loch, C. M., Eddins, M. J., and Strickler, J. E. (2011) Protein microarrays for the identification of praja1 e3 ubiquitin ligase substrates. *Cell Biochem Biophys* 60, 127-135.

48.   Stork, O., Stork, S., Pape, H. C., and Obata, K. (2001) Identification of genes expressed in the amygdala during the formation of fear memory. *Learn Mem* 8, 209-219.

49.   Xu, L., Sowa, M. E., Chen, J., Li, X., Gygi, S. P., and Harper, J. W. (2008) An FTS/Hook/p107(FHIP) complex interacts with and promotes endosomal clustering by the homotypic vacuolar protein sorting complex. *Mol Biol Cell* 19, 5059-5071.

50.   Richardson, S. C., Winistorfer, S. C., Poupon, V., Luzio, J. P., and Piper, R. C. (2004) Mammalian late vacuole protein sorting orthologues participate in early endosomal fusion and interact with the cytoskeleton. *Mol Biol Cell* 15, 1197-1210.

51.   Zheng, Q., Li, J., and Wang, X. (2009) Interplay between the ubiquitin-proteasome system and autophagy in proteinopathies. *Int J Physiol Pathophysiol Pharmacol* 1, 127-142.

52.   Naviglio, S., Mattecucci, C., Matoskova, B., Nagase, T., Nomura, N., Di Fiore, P. P., and Draetta, G. F. (1998) UBPY: a growth-regulated human ubiquitin isopeptidase. *EMBO J* 17, 3241-3250.

25

53.   Balut, C. M., Loch, C. M., and Devor, D. C. (2011) Role of ubiquitylation and USP8-dependent deubiquitylation in the endocytosis and lysosomal targeting of plasma membrane KCa3.1. *FASEB J* 25, 3938-3948.

54.   Niendorf, S., Oksche, A., Kisser, A., Lohler, J., Prinz, M., Schorle, H., Feller, S., Lewitzky, M., Horak, I., and Knobeloch, K. P. (2007) Essential role of ubiquitin-specific protease 8 for receptor tyrosine kinase stability and endocytic trafficking in vivo. *Mol Cell Biol* 27, 5029-5039.

55.   Berlin, I., Higginbotham, K. M., Dise, R. S., Sierra, M. I., and Nash, P. D. (2010) The deubiquitinating enzyme USP8 promotes trafficking and degradation of the chemokine receptor 4 at the sorting endosome. *J Biol Chem* 285, 37895-37908.

56.   Hasdemir, B., Murphy, J. E., Cottrell, G. S., and Bunnett, N. W. (2009) Endosomal deubiquitinating enzymes control ubiquitination and down-regulation of protease-activated receptor 2. *J Biol Chem* 284, 28453-28466.

57.   Hislop, J. N., Henry, A. G., Marchese, A., and von Zastrow, M. (2009) Ubiquitination regulates proteolytic processing of G protein-coupled receptors after their sorting to lysosomes. *J Biol Chem* 284, 19361-19370.

58.   Hengartner, M. O. (2000) The biochemistry of apoptosis. *Nature* 407, 770-776.

59.   Kumar, S. (2007) Caspase function in programmed cell death. *Cell Death Differ* 14, 32-43.

60.   Snigdha, S., Smith, E. D., Prieto, G. A., and Cotman, C. W. (2012) Caspase-3 activation as a bifurcation point between plasticity and cell death. *Neuroscience Bulletin* 28, 14-24.

61.   Williams, D. W., Kondo, S., Krzyzanowska, A., Hiromi, Y., and Truman, J. W. (2006) Local caspase activity directs engulfment of dendrites during pruning. *Nat Neurosci* 9, 1234-1236.

62. Lu, C., Fu, W., Salvesen, G. S., and Mattson, M. P. (2002) Direct cleavage of AMPA receptor subunit GluR1 and suppression of AMPA currents by caspase-3: implications for synaptic plasticity and excitotoxic neuronal death. *Neuromolecular Med* 1, 69-79.

63. Li, Z., Jo, J., Jia, J. M., Lo, S. C., Whitcomb, D. J., Jiao, S., Cho, K., and Sheng, M. (2010) Caspase-3 Activation via Mitochondria Is Required for Long-Term Depression and AMPA Receptor Internalization. *Cell* 141, 859-871.

64. Harvey, K. F., and Kumar, S. (1999) Nedd4-like proteins: an emerging family of ubiquitin-protein ligases implicated in diverse cellular functions. *Trends in Cell Biology* 9, 166-169.

65. Hu, N. W., Ondrejcak, T., and Rowan, M. J. (2012) Glutamate receptors in preclinical research on Alzheimer's disease: update on recent advances. *Pharmacol Biochem Behav* 100, 855-862.

66. Byers, B., Lee, H. L., and Pera, R. R. (2012) Modeling Parkinson's Disease Using Induced Pluripotent Stem Cells. *Current Neurology and Neuroscience Reports* 12, 237-242.

67. Kaczmarek, A., Vandenabeele, P., and Krysko, D. V. (2013) Necroptosis: the release of damage-associated molecular patterns and its physiological relevance. *Immunity* 38, 209-223.

68. Moujalled, D. M., Cook, W. D., Okamoto, T., Murphy, J., Lawlor, K. E., Vince, J. E., and Vaux, D. L. (2013) TNF can activate RIPK3 and cause programmed necrosis in the absence of RIPK1. *Cell Death & Disease* 4.

69. Coupienne, I., Fettweis, G., Rubio, N., Agostinis, P., and Piette, J. (2011) 5-ALA-PDT induces RIP3-dependent necrosis in glioblastoma. *Photochem Photobiol Sci* 10, 1868-1878.

70. Kumar, S., Tomooka, Y., and Noda, M. (1992) Identification of a set of genes with developmentally down-regulated expression in the mouse brain. *Biochem Biophys Res Commun* 185, 1155-1161.

71. Ingham, R. J., Gish, G., and Pawson, T. (2004) The Nedd4 family of E3 ubiquitin ligases: functional diversity within a common modular architecture. *Oncogene* 23, 1972-1984.

72.   Schwarz, L. A., Hall, B. J., and Patrick, G. N. (2010) Activity-dependent ubiquitination of GluA1 mediates a distinct AMPA receptor endocytosis and sorting pathway. *J Neurosci* 30, 16718-16729.

73.   Lin, A., Hou, Q., Jarzylo, L., Amato, S., Gilbert, J., Shang, F., and Man, H. Y. (2011) Nedd4-mediated AMPA receptor ubiquitination regulates receptor turnover and trafficking. *J Neurochem* 119, 27-39.

Figure Legends:

Figure 1: Subcellular Fractionation and Validation of Fractions

(A) A schematic of the subcellular fractionation protocol used to generate PSD fractions from the striata of animals treated with either saline or escalating doses of morphine for 5 days (adapted from (27)). TX-100, Triton X-100; PSD, postsynaptic density; PRE, presynaptic density. **(B)** Biochemical validation of the PSD fractions was carried out by Western blot analysis using antibodies to synaptophysin, a presynaptic marker, and to PSD-95, a postsynaptic marker and equal amounts (15 µg) of protein from striatal homogenates and PSD fractions as described in Experimental Procedures. A signal for PSD-95 but not for synaptophysin is seen in the PSD fractions.

Figure 2: Representative Figure Showing Differential Isotopic Labeling and LC-MS/MS.

Representative data for a downregulated protein, synaptopodin (**A**) and an upregulated protein, Gαo is shown (**B**). **(Left panel)** Bar graph of the normalized intensities of the iTRAQ reporter ions for a peptide fragment; **(Middle panel)** the continuous series of the b- and y-ions used for the identification of the peptide fragment; **(Right panel)** bar graph showing the ratio as Mean ± SD of the iTRAQ labels in relation to iTRAQ-113 signals obtained from all of the peptides derived from the protein.

Figure 3: Biochemical Validation of Proteins Shown to be Upregulated by Quantitative Proteomics.

PSD fractions (15 µg protein) from morphine or saline treated animals were subjected to Western blot analysis using antibodies to either Gαo, Gβ1, calcineurin B, neuromodulin (GAP43), annexin VI or Hsp70 as described in Experimental Procedures. Representative blot is shown in the figure. Data represent Mean ± SE of 4 independent animals. *p<0.05; **p<0.01; t-test.

Figure 4: Biochemical Validation of USP8, a Protein Shown to be Downregulated by Quantitative Proteomics.

PSD fractions (15 µg protein) from morphine or saline treated animals were subjected to Western blot analysis using antibodies to USP8 (**A**) as described in Experimental Procedures. The total level of ubiquitinated proteins (**B**) was assessed using anti-ubiquitin antibodies. Representative blot is shown in the figure. Data represent Mean ± SE of 4 independent animals. *p<0.05; **p<0.01; t-test.

Figure 5: Enrichment analysis of significantly upregulated and downregulated proteins.

Enrichr (29) was used to perform enrichment analysis on the significantly upregulated (**A**) and downregulated (**B**) proteins (24 were upregulated and 10 were downregulated in morphine treated samples) as described in Experimental Procedures. The proteins were first mapped to gene symbols and then used as input for Enrichr. The figure shows the canvas representation of the results.

Figure 6: Network Representation of Proteins Altered by Morphine Treatment Generated Using Intermediates from a Background Dataset.

Genes2FANS (30, 38) was used to connect the upregulated proteins (green) with the downregulated proteins (red) from the seed list using a maximum of two intermediates from the background literature-based PPI network. The network contains a total of 99 proteins and 180 interactions. Significant intermediates are shown in orange (z-score > 2.5). Upregulated proteins (green): CD81, CD81 protein; CLDN11, Claudin-11; GAP43, Neuromodulin; GNAO1, Guanine nucleotide-binding protein G(o) subunit alpha; GNB1, Guanine nucleotide-binding protein G(i)/ G(s)/G(t) subunit beta-1; GNB2, Guanine nucleotide-binding protein G(i)/ G(s)/G(t) subunit beta-2; PPP3R1, Calcineurin subunit B type 1; RAP1B, Ras-related protein Rap-1b; RPL18A, 60S ribosomal protein L18a; RPS24, 40S ribosomal protein S24; TNX, Thioredoxin. Downregulated proteins (red): DNAJB5, DnaJ homolog subfamily B member 5; LIMA1, LIM domain and actin-binding protein 1; PAK6, Serine/threonine-protein kinase PAK6; PJA1, E3 ubiquitin-protein ligase Praja-1; TRAF3, TNF receptor-associated factor 3; USP8, Ubiquitin carboxyl-terminal hydrolase 8. Significant intermediates (orange): ADRA2A, Alpha-2A adrenergic receptor; ADRBK1, Beta-adrenergic receptor kinase 1; AKT1, Protein kinase B alpha; CALM3, Calmodulin-3; CASP3, Caspase-3; GNG2, Guanine nucleotide-binding protein G(i)/ G(s)/G(o) subunit gamma-2; GRM7, Metabotropic glutamate receptor 7; HD4C4, Histone deacetylase 4; IKBKG, NF-kappa B essential modulator (NEMO); MAP3K14, Mitogen-activated protein kinase kinase kinase 14; MAP3K3, Mitogen-activated protein kinase kinase kinase 3; MAP3K5, Mitogen-activated protein kinase kinase kinase 5; NEDD4, E3 ubiquitin-protein ligase NEDD4; NFKB2, Nuclear factor NF-kappa B p100 subunit; OPRD1, Delta type opioid receptor; OPRk1, Kappa type opioid receptor; OPRL1, Nociceptin receptor; OPRM1, Mu type opioid receptor; RIPK3, Receptor-interacting serine/threonine protein kinase 3; RNF128, E3 ubiquitin protein ligase RNF128; RNF41, E3 ubiquitin protein ligase NRDP1; SPTBN1, Spectrin beta chain, non-erythrocytic 1; TSPAN4, Tetraspanin-4; UBC, Ubiquitin-conjugating enzyme; YWHAZ, 14-3-3 protein zeta/delta.

30

Figure 7. Biochemical Validation of Predicted Proteins from Network Analysis. Synaptosomal fractions (15 µg protein) from morphine or saline treated animals were subjected to Western blot analysis using antibodies to either RIPK3 (**A**), caspase-3 (**B**) or NEDD4 (**C**) as described in Experimental Procedures.

Table 1. Seed list of 25 Striatal PSD Proteins Upregulated by Morphine Treatment.

Full Name	Acc. #	Gene I.D.	M.W. (kDa)	Ratio (M/S)	p-value
Similar to cytochrome B-C1 complex, subunit 9	B2RYX1	UQCR10	7	1.4	0.001
Claudin-11	Q99P82	CLDN11	22	1.3	0.05
Guanine nucleotide-binding protein Gαo	F1LN36	GNAO1	21	1.3	0.001
40S ribosomal protein S26	D3Z8D7	RPS26	13	1.2	0.001
G-protein β2 subunit (Fragment)	Q91XL4	GNB2	24	1.2	0.001
40S ribosomal protein S24	D4ACJ1	RPS24	15	1.2	0.01
CD81 antigen	Q62745	CD81	26	1.2	0.01
Guanine nucleotide-binding protein β1 (Fragment)	Q45QL8	GNB1	28	1.2	0.01
Heat shock 70 kDa protein 1A/1B	Q07439	HSPA1A/B	70	1.2	0.01
Ras-related protein Rap-1b	Q62636	RAP1B	21	1.2	0.01
Similar to isoform 2 of protein XRP2	D3ZTJ0	XRP2	43	1.2	0.02
Similar to leucine zipper protein 1	D3ZWV9	LUZP1	119	1.2	0.02
Ubiquitin-like modifier-activating enzyme ATG7	D3ZP91	ATG7	77	1.2	0.02
Glutathione S-transferase Mu 5	Q9Z1B2	GSTM5	27	1.2	0.03
Protein kinase, AMP-activated, β2 non-catalytic subunit	G3V9X3	PRKAB2	30	1.2	0.03
Thioredoxin	P11232	TXN	12	1.2	0.03
TNF receptor-associated factor 3	D3Z9G0	TRAF3	64	1.2	0.03
60S ribosomal protein L18a (Fragment)	F1M0K6	RPL18A	21	1.2	0.04
60S ribosomal protein L21	D3ZPN7	RPL21	19	1.2	0.04
Calcineurin subunit B, Type 1	F1M522	PPP3R1	18	1.2	0.04
WD repeat-containing protein 41	B2RYI7	WDR41	51	1.2	0.04
L-asparaginase	Q8VI04	ASRGL1	34	1.2	0.05
Neuromodulin	P07936	GAP43	24	1.2	0.05
Similar to annexin-6 (Mus musculus)	D4ABR6	ANXA6	75	1.2	0.05

Striatal PSD proteins from saline and morphine treated animals (n= 4/group) were subjected to proteomics analysis and quantified as described in Experimental Procedures. Acc. #, accession number; M/S, morphine/saline.
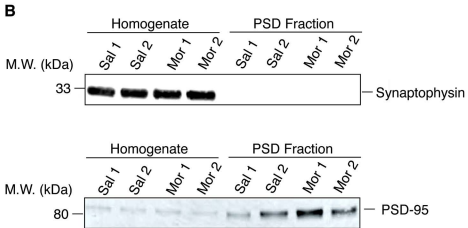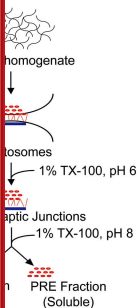
Table 2: Seed list of 13 Striatal PSD Proteins Downregulated by Morphine Treatment.

Full Name	Acc. #	Gene I.D.	M.W. (kDa)	Ratio (M/S)	p-value
EST Domain-containing transcription factor ERF	D3ZJW0	ERF	59	0.8	0.01
FTS and Hook interacting protein	D4A7B7	FAM160A2	99	0.8	0.02
Opioid growth factor receptor	D4ABV6	OGFR	63	0.8	0.02
Similar to E3 ubiquitin-protein ligase Praja-1	Q66HF7	PJA1	45	0.8	0.03
Synaptopodin	Q9Z327	SYNPO	100	0.8	0.03
Ubiquitin carboxyl-terminal hydrolase	D3ZN39	USP8	124	0.8	0.03
Serine/threonine protein kinase PAK6	D3ZQ51	PAK6	75	0.8	0.03
Protein Lima1	F1LR10	LIMA1	83	0.3	0.03
CST complex subunit STN1	Q6AYD2	OBFC1	47	0.8	0.05
Dnajb5 protein (Fragment)	B2GV48	DNAJB5	44	0.8	0.05

Striatal PSD proteins from saline and morphine treated animals (n= 4/group) were subjected to proteomics analysis and quantified as described in Experimental Procedures. Acc. #, accession number; M/S, morphine/saline.

Table 3: Significant Intermediates from the Background Dataset That Link Seed List Proteins.

Intermediate Nodes	Protein Name	Intermediate Nodes	Protein Name
ABL1	Tyrosine protein kinase ABL1	MAPK1	Mitogen-activated protein kinase 1
ACTN4	α-actinin 4	MAPK3	Mitogen-activated protein kinase 3
ADRA2A	α2A adrenergic receptor	MAPT	Microtubule-associated protein tau
ADRBK1	β-adrenergic receptor kinase 1	MATR3	Matrin 3
AKT1	RAC-α serine/threonine protein kinase	NEDD4	E3 ubiquitin protein ligase NEDD4
APLP2	Amyloid-like protein 2	NFKB2	Nuclear facto NF-κ-B p100 subunit
ARRB1	β-arrestin 1	NSF	Vesicle-fusing ATPase
ARRB2	β-arrestin 2	OPRD1	δ type opioid receptor
CACNA1A	Voltage-dependent P/Q type calcium channel subunit α1A	OPRM1	μ type opioid receptor
CACNA1C	Voltage-dependent L type calcium channel subunit α1C	PA2G4	Proliferation-associated protein 2G4
CALM1	Calmodulin	PACSIN1	Protein kinase C and casein kinase substrate in neurons protein 1
CAND1	Cullin-associated NEDD8-dissociated protein 1	PARP1	Poly [ADP-ribose] polymerase 1
CASP3	Caspase-3	PLEC	Plectin
CCT7	T-complex protein 1 subunit η	PPP3CA	Serine/threonine-protein phosphatase 2B catalytic subunit α isoform
COPS6	COP9 signalosome complex subunit 6	PPP3CB	Serine/threonine-protein phosphatase 2B catalytic subunit β isoform
CSNK1A1	Casein kinase I isoform α	PRKAA1	5'-AMP-activated protein kinase catalytic subunit α1
CTBP1	C-terminal binding protein 1	PRKCA	Protein kinase C α type
CTNNB1	Catenin β1	PRKCD	Protein kinase C δ type
CUL2	Cullin-2	PRKCE	Protein kinase C ε type
CUL5	Cullin-5	PRNP	Major prion protein
DLG4	Disks large homolog 4	RAC1	Ras-related C3 botulinum toxin substrate 1
EWSR1	RNA-binding protein EWS	RAP1GAP	Rap1 GTPase-activating protein 1
FLNA	Filamin-A	RASA1	Ras GTPase-activating protein 1
FMR1	Fragile X mental retardation protein1	RASGRF1	Ras-specific guanine nucleotide-releasing factor 1

GABBR1	γ-aminobutyric acid type B receptor subunit 1	RB1CC1	RB1-inducible coiled-coil protein 1
GNAQ	Guanine nucleotide-binding protein Gαq	RGS6	Regulator of G-protein signaling 6
GNG2	Guanine nucleotide-binding protein Gi/Gs/Go subunit γ2	RNF128	E3 ubiquitin protein ligase RNF128
GOLGA2	Golgin subfamily A member 2	RNF41	E3 ubiquitin protein ligase NRDP1
GPX1	Glutathione peroxidase 1	RPS24	40S ribosomal protein S24
GRB2	Growth factor receptor-bound protein 2	RTN4	Reticulon-4
GRIN1	Glutamate receptor ionotropic, NMDA1	SPTAN1	Spectrin α chain, non-erythrocytic 1
GRIN2A	Glutamate receptor ionotropic, NMDA 2A	SPTBN1	Spectrin β chain, non-erythrocytic 1
GRIN2B	Glutamate receptor ionotropic, NMDA 2B	SQSTM1	Sequestosome-1
GRM7	Metabotropic glutamate receptor 7	SRC	Proto-oncogene tyrosine protein kinase Src
GSK3B	Glycogen synthase kinase 3β	SRR	Serine racemase
GSN	Gelsolin	STAU1	Double-stranded RNA-binding protein Staufen homolog 1
HDAC2	Histone deacetylase 2	SYN1	Synapsin-1
HDAC4	Histone deacetylase 4	TBK1	Serine/threonine protein kinase TBK1
HDAC5	Histone deacetylase 5	TJP1	Tight junction protein ZO-1
HNRNPA2B1	Heterogeneous nuclear ribonucleoproteins A2/B1	TP53	Cellular tumor antigen p53
HSP90AA1	Heat shock protein HSP 90α	TSPAN4	Tetraspanin-4
HSPA5	78 kDa glucose-regulated protein	TSSC1	Protein TSSC1
HTT	Sodium-dependent serotonin transpoter	UBC	E2 Ubiquitin-conjugating enzyme
IKBKG	NF-κ-B essential modulator	ULK1	Serine/threonine protein kinase ULK1
ITPR1	Inositol 1,4,5-triphosphate receptor type 1	UNC119	Protein unc-119 homolog A
KRT10	Keratin, type I cytoskeletal 10	VCL	Vinculin
LRRC4	Leucine-rich repeat-containing protein 4	VIM	Vimentin
MAP2K4	Dual specificity mitogen-activated protein kinase kinase 4	YWHAB	14-3-3 protein β/α
MAP3K14	Mitogen-activated protein kinase kinase kinase 14	YWHAQ	14-3-3 protein θ
MAP3K3	Mitogen-activated protein kinase kinase kinase 3	YWHAZ	14-3-3 protein ζ/δ
MAP3K5	Mitogen-activated protein kinase kinase kinase 5		

A binomial proportions test (z-score) was used to identify the intermediates that had higher preference to interact with proteins from the seed list as compared to the background PPI network. Proteins with a z-score > 2.5 were designated as significant intermediates and with a z-score < 2.5 as other intermediates.
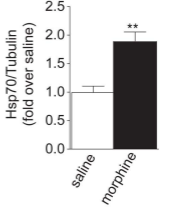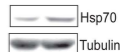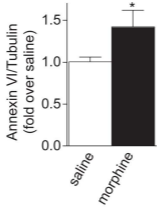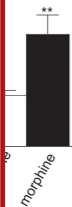
36

B

Homogenate | PSD Fraction

M.W. (kDa)
Sal 1 | Sal 2 | Mor 1 | Mor 2 | Sal 1 | Sal 2 | Mor 1 | Mor 2

33 ─ ─ Synaptophysin

Homogenate | PSD Fraction

M.W. (kDa)
Sal 1 | Sal 2 | Mor 1 | Mor 2 | Sal 1 | Sal 2 | Mor 1 | Mor 2

80 ─ ─ PSD-95

homogenate

1% TX-100, pH 6

tosomes

Synaptic Junctions

1% TX-100, pH 8

PRE Fraction
(Soluble)

B. T-A-R-P-F-G-Mox-Q-S-P-G-T-T-S-Q-I-E-Q-S-P-M-M-G-R
b1 b2 b3 b5 b6 b7 b8   y17 y16 y15 y14   y12 y11 y10 y9 y7 y6 y5 y3 y2 y1

C.

E. MOX-H-E-S-L-M-L-F-D-S-I-C-N-N-K
b1 b2 b3 b4 b5 b6 b7 b9   y4 y3 y2 y1

F.

B
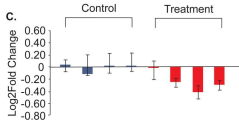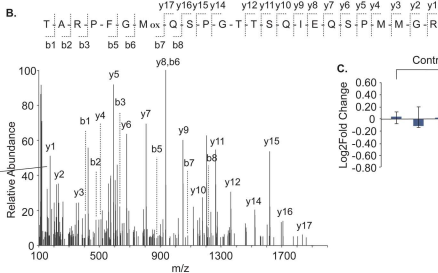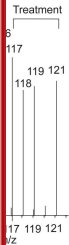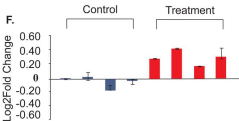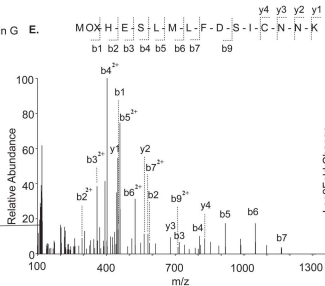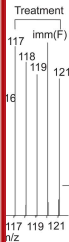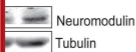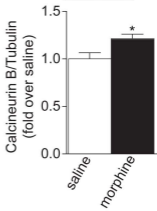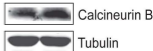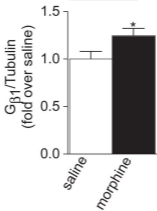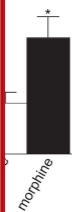
USP8

Tubulin

Ubiquitin

Tubulin

Ubiquitin/Tubulin (fold over saline)

**

Saline   Morphine

A ...ammalian Phenotype

B MGI Mammalian Phenotype

Abnormal Neuronal Functions

7
6
5
4 3 2
1
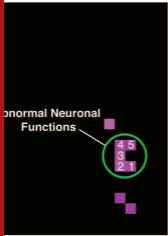
...l eye electrophysiology
...l neuron morphology
...l nervous system
...l brain morphology
...l motor capabilities
...l social behavior

1. Abnormal synaptic transmission
2. Abnormal emotion/affected behavior
3. Abnormal motor capabilities
4. Abnormal brain morphology
5. Abnormal nervous system
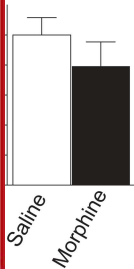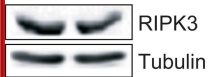6. Abnormal learning/memory
7. Abnormal social behavior

Reactome

Opioid Signaling

Human Gene Atlas

Pineal Day/Night

MicroRNAs

...5, MIR-32, MIR-92,
...R-363, MIR-367

MIR-485-3P

ENCODE

CTCF

Fig. 6

B.

C.